Intramolecular Charge Transfer (ICT) and Solvation of a Rigidly Linked Pyrene/*N*-Methylindolino Derivative and Related Compounds in Linear Alcohols

A. Wiessner,[†] W. Kühnle, T. Fiebig, and H. Staerk*

Max-Planck-Institut für biophysikalische Chemie, Abteilung Spektroskopie und Photochemische Kinetik, Am Fassberg 11, D-37077 Göttingen, Germany

Received: April 24, 1996; In Final Form: July 17, 1996[⊗]

Measurements on a rather rigid and coplanar bichromophoric compound have been carried out with respect to intramolecular charge separation, as well as regarding solvation and lifetime of the CT state in alcohol solutions. The results indicate that the CT step proceeds very efficiently followed by a Stokes shift of the CT emission band governed by the dielectric relaxation of the solvent (a series of *n*-alcohols). The average Stokes-shift time, τ_{solv} (of a few hundred picoseconds), correlates directly with the longitudinal relaxation time, $\tau_L = (\epsilon_\infty/\epsilon_s)\tau_D$, of the solvent. The recently developed single-shot spectrostreak picosecond technique was used for the collection of the time-resolved emission spectra.

I. Introduction

The causes for a time-dependent Stokes shift of a charge transfer (CT) emission band can be both intramolecular reorganizations and solvation of the CT dipole by the surrounding solvent. These two processes can only be separated by the choice of a largely rigid probe molecule. In order to exclude intramolecular rotations, we chose compound **4** (Figure 1), which was synthesized in this laboratory. It allows us to study consecutive processes—following "instantaneous" charge separation—in the absence of interfering intramolecular dynamics. Molecules **1**−**3**, having different intramolecular mobility, served as reference compounds. They are referred to just to compare briefly some relevant and interesting spectral and kinetic properties. In the past, few fluorescent systems with intramolecular charge separation have been studied in which the donor and acceptor moieties are separated by saturated rigid spacers.[1,2]

A. Solvent Relaxation. Various theories deal with the relaxation of polar solvents. According to the simplest one, the continuum theory, the solvent is described as a structureless dielectric continuum in which the molecules do not interact among each other. In the case of a solvent that can be described by a single Debye dispersion region as

$$\epsilon^*(\omega) = \epsilon_\infty + \frac{\epsilon_s - \epsilon_\infty}{1 + i\omega\tau_D} \tag{1}$$

this is expected to lead to a monoexponential relaxation, e.g., of the dynamic Stokes shift function, $S(t)$ (compare eq 7), with time constant

$$\tau_L = \frac{\epsilon_\infty}{\epsilon_s}\tau_D \tag{2}$$

the so-called longitudinal dielectric relaxation time, where τ_D is the Debye time. In this equation, the structure of the solute molecule is not taken into consideration. For dipoles, the equation requires modification, and the dielectric constant, ϵ_c, within the sphere to be solvated must be considered,[3] which

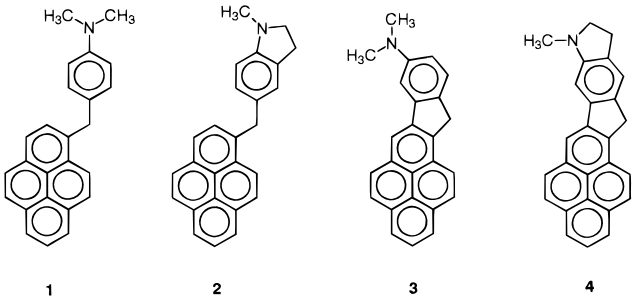

Figure 1. Structures of compounds used in this study. **1**, dimethyl-(4-pyren-1-ylphenyl)amine; **2**, 1-methyl-5-pyren-1-yl-2,3-dihydro-1*H*-indole; **3**, 8-*N*,*N*-(dimethylamino)-11*H*-indeno[2,1-*a*]pyrene; **4**, 8-methyl-8,9,10,12-tetrahydrophenaleno[1′,9′:4,5,6]indeno[2,1-*f*]indole.

leads to an exponential decay with $\tau_{LD} \neq \tau_L$:

$$\tau_{LD} = \frac{2\epsilon_\infty + \epsilon_c}{2\epsilon_s + \epsilon_c} \tag{3}$$

For the sake of simplification, ϵ_c is often set equal to 1.[3−5] τ_{LD} times calculated by (3) for medium and highly polar solvents are systematically ca. 20% larger than τ_L. If the solvent does not follow a Debye behavior and must be described by several dispersion regions, a multiexponential behavior is obtained with τ_L or τ_{LD} times calculated in analogy to eq 2 or 3, respectively. Since the continuum theory ignores the molecular structure of the solvent, it therefore often does not provide a satisfactory description of the experimentally observed relaxation phenomena.

The mean spherical approximation (MSA)[6−8] describes both the solvent and the solute molecule as hard spheres with either a point charge or a point dipole in the center. This approximation predicts a nonmonoexponential solvation behavior since the inner solvation shell and the more distant shells have to be treated differently. The inner shell is disturbed by the presence of the solute and has a relaxation time, τ_G, which depends on the ratio of the solvent molecule radius, D_s, and the radius, r_c, of the solute:

* Author to whom correspondence should be addressed.
[†] Now with Max-Planck-Institut für Mikrostrukturphysik, 06120 Halle/Saale, Germany.
[⊗] Abstract published in *Advance ACS Abstracts,* December 15, 1996.

S1089-5639(96)01182-6 CCC: $14.00

$$\tau_G = \tau_D \frac{1 + \frac{1}{2}\frac{r_c}{D_s}(\epsilon_\infty + 3)}{1 + \frac{1}{2}\frac{r_c}{D_s}(\epsilon_s + 3)} \quad (4)$$

The more distant solvent relaxes with τ_L. The solvation should therefore proceed at least biexponentially with time constants between τ_L and τ_D, whereby the inner shell relaxes more slowly than the remaining solvent (Onsager "inverted snowball" model[9]). τ_L sets the lower limit of the relaxation times; shorter time components should not appear. This theory, however, only holds for nonassociating solvents. It fails for associating solvents, because specific interactions, e.g., the formation of hydrogen bonds, as is the case in alcohols, are not taken into account. Thus far, only initial attempts of a theoretical treatment exist for alcohols, and these attempts are directed merely at smaller alcohols such as methanol and ethanol. Alcohols are usually described by three Debye dispersion regions. The longest time (τ_{L1}) is attributed to the rotation of solvent clusters, the medium time (τ_{L2}) to the rotation of free solvent molecules, and the shortest time (τ_{L3}) to the rotation of OH dipoles (describing a cone). By far the greatest influence on the relaxation in neat solvents comes from τ_{L1}. However, in the immediate vicinity of the solute, a breaking of the solvent structure is expected:[8] The number of hydrogen bonds is drastically reduced so that the molecules in the solvation shell nearest to the solute can behave almost like free molecules which relax with a relaxation time approximating τ_{L2}. Contrary to the MSA theory for nonassociating solvents, the innermost solvent shell would relax faster than the more distant solvent molecules. This must lead to a multiexponential relaxation with time components between τ_{D2} and τ_{D1}. The influence and the contribution from the OH-dipole rotation, however, are not elucidated by this model. Furthermore, no account is taken of possible specific interactions between solvent and solute.

Alternatively, another suggestion was advanced which considers the influence of translational movements of solvent molecules.[10,11] This also leads to at least biexponential behavior. Unfortunately, no data exist presently for translational diffusion in alcohols.

B. Solvation of Polar Solute Molecules. A variety of different measurements of solvation processes have been described in the literature.[12−15] In most cases, these measurements were carried out on molecules having strongly different dipole moments in the ground and excited states e.g., coumarins, rhodamines, and DMABN ((dimethylamino)benzonitrile). All authors found nonmonoexponential solvation dynamics. The solvation times had been compared with the different theoretically determined relaxation times (eqs 1−4). Dependent on the solvent used, agreements with different theoretical relaxation times were found.

Rullière and Declemy[13] investigated the solvation of a rigid probe molecule in the solvents dimethylformamide and propylene carbonate. They found an agreement of the solvation time with the so-called molecular relaxation time, τ_M,[16,17] defined as

$$\tau_M = \frac{2\epsilon_s + \epsilon_\infty}{3\epsilon_s g_k}\tau_D \quad (5)$$

with g_k being the Kirkwood factor[18] of the solvent. Faster components of the solvation dynamics could not be detected due to the time resolution limit of ca. 40 ps.

Maroncelli and Fleming[12] investigated the solvation behavior and the influence of the solvent on the probe molecule coumarin 153. In addition to diverse nonpolar to strongly polar solvents, these authors also used *n*-alcohols (from methanol to butanol) which showed a different behavior compared to other solvents, with respect both to the static and the dynamic properties. These differences were partly attributed to the ability of the alcohols to form hydrogen bonds (see above). In all solvents, the solvation times deviated from the predictions of the continuum theory, the deviations increasing with increasing polarity. The deviation from monoexponentiality was attributed to the different behavior of the various solvation shells.

Barbara et al.[14,15] carried out measurements in a variety of solvents (short-chain alcohols, alkyl nitriles, water, etc.) with coumarins as the probe substance. They found a relatively good agreement of the averaged solvation times with τ_L as predicted by the continuum theory.

The differing results obtained by the above authors point out that a satisfactory agreement has not been reached between calculated and measured relaxation times for all solvents as a group. The longer chain *n*-alcohols used in the present work are characterized by only a few relatively imprecise measurements,[19] leaving the solvation behavior in such solvents as a continuing open question.

II. Experimental Section

A. Synthesis and Characterization of Compounds 3 and 4. Because of confusing structure suggestions in the literature with respect to compounds **3** and **4** with rigid spacer, it is indispensable to report briefly on their preparation, synthesis, and characterization in our laboratory.

The preparation of compound **3**—and similarly compound **4**—has been carried out according to the scheme in Figure 2.

Vollmann et al.[20] and Clar[21] interpreted the ring-closure reaction (in the case R = H) as a linkage of the phenyl ring (ortho position) with position 10 of pyrene, leading to IIb. Vollmann et al.[20] converted the product as received into pyrenylbenzoic acid by reaction with fused alkali. In the following step, they transformed the pyrenylbenzoic acid with $Ba(OH)_2$ into phenylpyrene, which had a melting point of 169 °C. However, these investigators erroneously named this product 4-phenylpyrene. Jutz et al.[22] showed that 169 °C is actually the melting point of 2-phenylpyrene[23] instead of the 4-substituted pyrene derivative. Further proof was provided by Dickermann and Feigenbaum,[24] who compared the IR spectra of several ketone derivatives (similar to IIa and IIb) and concluded the five-membered-ring formation in the reaction originally made by Vollmann et al.[20]

Figure 3 shows part of the 300-MHz NMR spectrum of III (R = $N(CH_2)_3$) in $CDCl_3$. As ^1H NMR data of pyrene derivatives are well-known from the literature,[25] we suggest the following interpretation: The isolated singlet at 8.5 ppm is attributed to H-6. The doublet at 8.21 ppm belongs to H-12; the observed coupling between H-12 and H-13 (J = 9 Hz) is equal to the corresponding one in 1-substituted pyrene derivatives. However, a doublet signal that would have been expected for H-2 (compare numbering in structure I, Figure 2) between approximately 7.80 and 7.90 ppm is totally missing. Therefore, we maintain strong agreement with refs 22−24, namely, that the rigid compounds are structurally related to IIa instead of IIb.

B. Stability Tests of the Compounds. Stability tests of the compounds reveal the following results: Compounds **3** and **4** oxidize rapidly (**3** → IIa with a lower rate, **4** with a higher rate to the corresponding ketone). During irradiation with UV

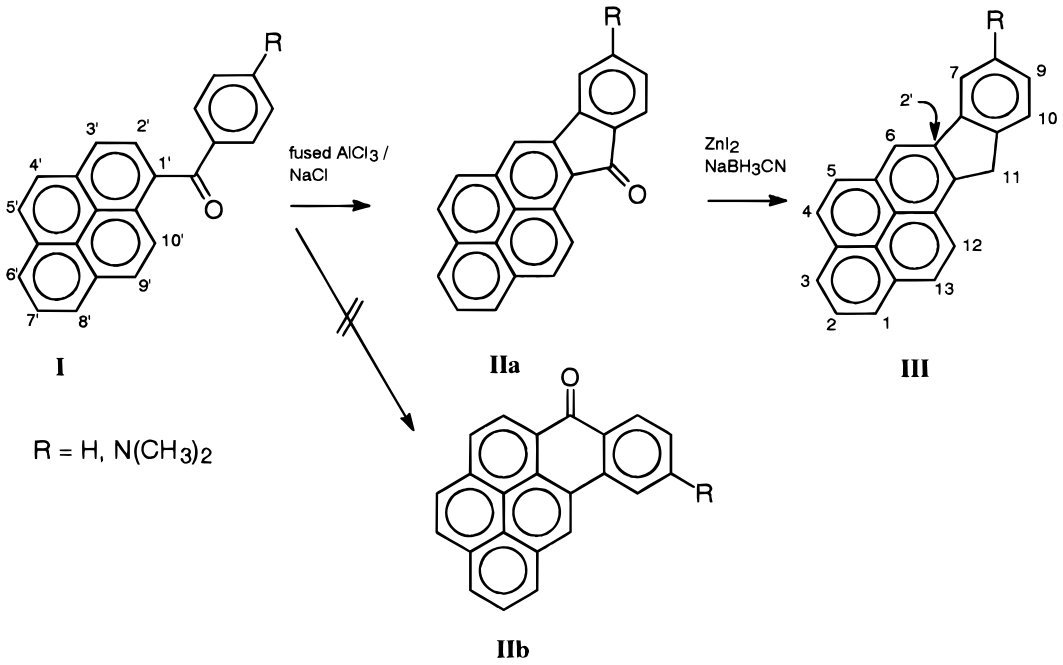

Figure 2. Synthesis steps leading to compounds **3** and **4**, respectively. The precursor molecule is marked with primed numbers; official IUPAC numbering is applied with the final product molecule.

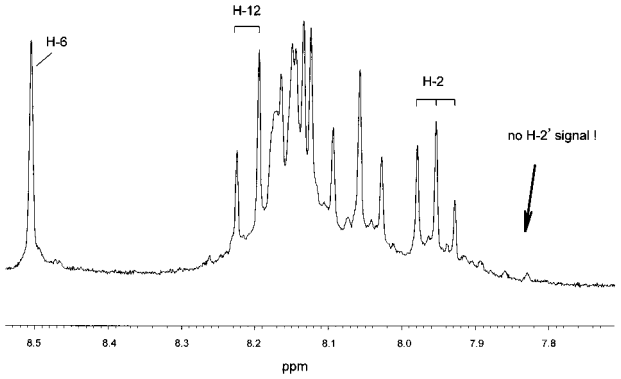

Figure 3. NMR (300 MHz) spectrum of **3** (III with R = $N(CH_2)_3$) in deuterated acetonitrile.

light, irreversible photodegradation takes place. This becomes manifest in the fluorescence spectrum by the appearance of a broad band at 430 nm accompanied by a decrease of the red emission intensity (e.g., at 650 nm in acetonitrile). Furthermore, we have demonstrated in separate experiments that the band at 430 nm can be significantly diminished upon addition of a base (e.g., lithium amide) while the intensity of the red band (650 nm) increased. We conclude from this observation that an amino group, protonated by residual water[26] (counteranion OH^-), is mainly responsible for the appearance of the weak blue band. After prolonged irradiation of a sample with **4** (HPLC prepared and degassed), the NMR spectrum did not show any typical H signal of substance **4**. Repeated preparation of fresh solutions was therefore necessary, and we strived for a low dose of light irradiation in all measurements described in this paper.

C. Apparatus. Samples were prepared via HPLC directly into the cuvette, followed by the usual freeze−pump−thaw procedure before sealing. For measuring time-resolved emission spectra the spectrostreak apparatus described previously[27] was used. It comprises a streak camera (Hamamatsu C 1370-01) with a self-designed grating objective,[27a] a CCD camera, and a Nd:glass or Nd:YAG laser for excitation. The time resolution of the entire spectrostreak arrangement (excitation pulse, 7 ps; grating, 4−15 ps; streak camera, 2 ps) is 9−16 ps. The temperature of the sample can be varied and controlled between −20 and 60 °C. Transient absorption spectra (TRABS) were determined in an apparatus with a time resolution (Nd:YAG laser) of ca. 45 ps,[28,29] which allows the recording of complete spectra over the wavelength range between 400 and 800 nm using a picosecond-white-light continuum at delay times from −200 to +9000 ps. The lifetime of the CT state was measured with a time-correlated single-photon-counting apparatus (Edinburgh Instruments). Stationary absorption spectra were obtained from an absorption spectrometer, Varian Cary 5e; stationary emission spectra were recorded with a Perkin-Elmer LS50, which was also deployed for determining the quantum efficiencies of CT emission with quinine bisulfate (CBS) in 0.1 N H_2SO_4 as the reference standard. CBS has a quantum efficiency of 0.51.[30] The area under the measured time-resolved spectra (spectrostreak technique) was calculated by fitting to a model function (so-called log-normal function[12,34]) and by extrapolation.

III. Results

A. Absorption and Excitation Spectra. The absorption spectrum of compound **4** in the range of the transitions $S_2 \leftarrow S_0$ (ca. 310−360 nm) is similar to that of methylpyrene (MePy). However, at the red end of the spectrum, the absorption−$S_1 \leftarrow S_0$−is increased and shifted toward 400−410 nm. We consider the S_1 state as a superposition of a pure localized pyrene state and a delocalized CT state. Substitution of the donor moiety DMA (dimethylaniline) in **3** by 1-methylindolino, leading to compound **4** (or in **1,** leading to **2**), does not exhibit significant changes of the absorption spectra (see also the spectra of **3** and **4** in *n*-hexane, displayed in Figure 11, below). In the solvents *n*-pentanol, *n*-hexanol, *n*-heptanol, and *n*-octanol, compound **4** shows only a slight red shift (∼1.5 nm) of the absorption bands with increasing polarity of the solvent, and significant changes of the band shape are absent. This observation points at only a negligibly different polarity of ground and first excited states. The excitation spectra are practically identical with the absorption spectra.

B. Emission Spectra. Figure 4 shows the emission spectra of compound **4** and of the reference compounds **1**, **2**, and **3** in

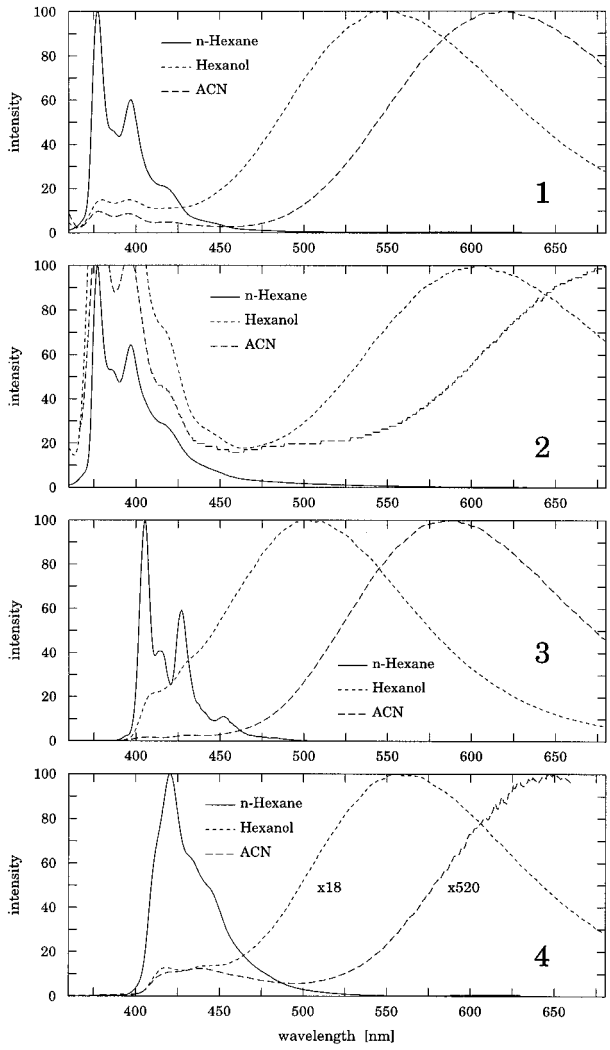

Figure 4. Normalized stationary emission spectra of **4** and of the reference compounds **1**, **2**, and **3** in the solvents *n*-hexane, hexanol, and acetonitrile. For the very weak band at 430 nm in **4**, particularly in acetonitrile, see text.

different solvents. Compound **4** in *n*-hexane has, compared to **1** (as well as to MePy—not shown), a strongly red-shifted band, and the vibrational structure can only be faintly recognized. From this relatively unstructured spectrum, one can also conclude that a more or less delocalized excited state (DE) prevails in the case of **4**, possibly mixed with a CT state, but not a pure exciplex. The shift of the emission spectrum in *n*-hexane is in accord with the position of the absorption spectrum; the short-wavelength edge of the emission overlaps with the long-wavelength band of the S_1 absorption and thus marks the 0−0 transition which is shifted to lower energies (cf. Figure 11).

In hexanol, by contrast, the CT emission is strongly red-shifted with a maximum at ca. 560 nm; the maximum in acetonitrile is found at about 650 nm. One explanation for such a strong Stokes shift may be the better donor property of the methylindoline moiety compared with the DMA moiety (cf. compound **3**), which results in a larger stabilization energy of the intramolecular CT state.

In summary, the comparison of compound **4** in different solvents (Figure 4, bottom) reveals the following particular features: The bands in hexanol and acetonitrile (ACN) are strongly red-shifted, as already mentioned. Their maximum intensities decrease with respect to *n*-hexane in the ratio 1:(1/12):(1/520). The shoulders (or extra bands) in hexanol and ACN

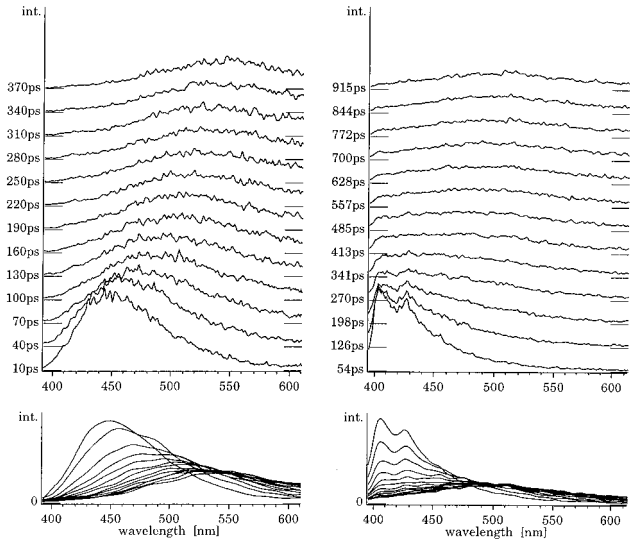

Figure 5. Spectrostreak measurements of compounds **4** (left) and **3** (right) in hexanol at room temperature (23 °C).

can be attributed to a small fraction of a deteriorated substance but clearly not to a locally (or delocalized) excited state. This has additionally been tested by lifetime studies; the measured long lifetime (much longer than the CT lifetime) seems to verify the appearance of pyrenyl-like fragments with inactive quencher moiety (see Experimental Section). The CT emission spectra in the three solvents, as pictured, show the expected behavior: The red-shift increases with increasing solvent polarity.

C. Spectrostreak Measurements. The spectrostreak measurement of compound **4** in *n*-hexanol at room temperature (Figure 5, left) shows only a CT emission band shifting to the red during a time (1/*e*) of about 190 ps. Emission from a locally excited state, which is expected to show an identifiable fluorescence below 430 nm, is not detected. One recognizes the intensity drop in the course of the band shift. On a wavenumber scale ($\tilde{\nu}$/cm^{-1}), the change of the emission intensity would appear less dramatic due to the necessary change of scale and intensity correction. Figure 5, right, displays spectrostreak measurements of compound **3** in hexanol for comparison. A strong emission of a band system between 400 and 450 nm is clearly recognized, which can be attributed to the locally excited state (cf. Figure 4.3). Electron-transfer kinetics and solvation dynamics proceed on similar time scales, and a separation of the two processes has not been possible to date.

For the evaluation of the signals, the obtained time-resolved spectra of **4** were fitted to a log-normal model function[12] on the wavenumber scale at fixed times. This fitting provides the actual maximum, the half-width, and the asymmetry factor of the emission band.

Time-Dependent Shift of the Emission Band. In order to determine the dynamic Stokes shift of **4**, measurements were carried out in *n*-pentanol, *n*-hexanol, *n*-heptanol, and *n*-octanol at −20, 0, 20, and 40 °C. The measurements lead to the empirical shift functions (correlation functions) $C(t)$ of the CT band maxima (peak wavenumbers) $\tilde{\nu}_p(t)$,

$$C(t) = \frac{\tilde{\nu}_p(t) - \tilde{\nu}_p(\infty)}{\tilde{\nu}_p(0) - \tilde{\nu}_p(\infty)} \qquad (6)$$

or $\tilde{\nu}_p(t) = C(t)(\tilde{\nu}_p(0) - \tilde{\nu}_p(\infty)) + \tilde{\nu}_p(\infty)$, which in most cases cannot be fitted monoexponentially. Therefore, we used the following relationship as the Stokes-shift function, $S(t)$:

$$S(t) = A_1 \exp\left(-\frac{t}{\tau_1}\right) + A_2 \exp\left(-\frac{t}{\tau_2}\right) + \tilde{\nu}_p(\infty) \qquad (7)$$

where $\tilde{\nu}_p(\infty)$ is the final $\tilde{\nu}$ value of the band maximum (suffix p for peak) corresponding to the relaxed CT state. This function, $S(t)$, was fitted to the measured values, $\tilde{\nu}_p(t)$. The calculated mean solvation time, $\langle\tau_s\rangle$, which was determined from the time constants, τ_i, and their pertinent amplitudes, A_i, by calculating the area under the decay curve according to $\langle\tau_s\rangle(A_1 + A_2) = A_1\tau_1 + A_2\tau_2$, correlates relatively well with the longitudinal relaxation time, τ_{L1}, of the solvent.

The results of such evaluations for the different solvents used in the present work are listed in Table 1 at the different temperatures. Most measurements could not be fitted monoexponentially. A multiexponentiality is particularly manifest at lower temperatures and in the case of *n*-pentanol. Additional data derived from the monoexponential fit whenever such a fit provided marginally acceptable results compared to the biexponential fit data are also listed in Table 1.

A comparison with the longitudinal relaxation time of the solvent indicates that the mean times are of the order of magnitude of τ_{L1} but are almost always shorter than τ_{L1}. The concurrence improves with increasing temperature. The plot of the mean shift times $\langle\tau_s\rangle$ against τ_{L1} for all solvents (Figure 6) shows that the correlation is independent of the selection of the solvent. It appears that the macroscopic parameter τ_{L1} is adequate to approximately describe the solvation behavior and that solvent-specific microscopic effects do not have to be invoked for elucidation.

Width of the Emission Band. During the shift of the emission band, a variation of the bandwidth is expected since the state of solvation is changing.[31] A linear variation, however, is unlikely. The width of the emission band increases by ca. 1000−1700 cm^{-1} during the solvation; a smaller change is generally observed at lower temperatures. The final width in all four solvents is between 5000 and 5500 cm^{-1}.

Emission Intensity as a Function of Time. It decreases during the CT band shift of several hundred picoseconds to about one-half, followed by a decrease with a much longer decay time (ca. 15 ns as determined with the photon-counting apparatus; cf. Tables 3 and 4). For several reasons, the intensity at the shifting maximum of the band is an inadequate measure for the population of the emitting CT state: From the fit of the model function (so-called log-normal function[12]) to the measured data, a variation of the band shape and the peak position, $\tilde{\nu}_p$, during the shift process results. In order to determine the population of the CT state, a band integration over the entire width of the CT band is necessary.[34] It should be noted that the emissive species must be conceived as a Hertz dipole with its emission probability increasing with $\tilde{\nu}^3$. At constant oscillator strength, the emission in the blue range of the spectrum will therefore be higher than in the red spectral region. Accordingly, band integration is carried out after the emission intensities have been divided by $\tilde{\nu}^3$.[12,34] This correction and summation over the extrapolated spectral range has been implemented for the different solvents and temperatures. Without $\tilde{\nu}^3$ correction, the integrated intensities indeed show a fast decay at early times, while following the $\tilde{\nu}^3$ correction the fast component is absent (cf. Figure 7). This result for compound **4** contributes to the question of whether the CT dipole fully evolves during the (in this example "slow") solvation process or whether the dipole moment remains constant after the primary charge separation event. A slow development of the dipole strength would result in a change of the oscillator strength for emission which, in turn, would lead to a significant intensity change of the corrected band integral. For compound **4**, such behavior could not be observed at any temperature with any of the solvents used in this investigation.

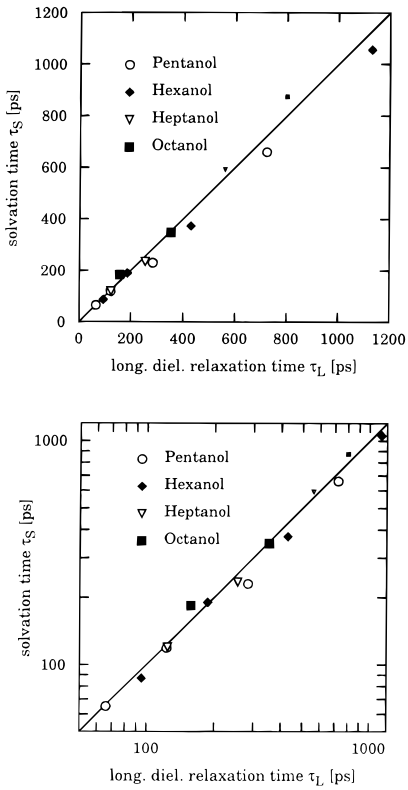

Figure 6. Comparison of the mean solvation times, τ_s, of **4** with τ_L. The smaller symbols indicate those values where an extrapolated value for τ_L had to be used. left, linear plot; right, log−log plot. The indicated line has a slope of 1.

TABLE 1: Correlation Time of the CT Emission as Obtained from the *C*(*t*) Function (eq 6) for Compound 4 in Linear Alcohols

solvent	temp/°C	$\tilde{\nu}_p$/cm^{-1}	monoexpon. fit, τ_s/ps	biexpon. fit, $\langle\tau_s\rangle^a$/ps	$\tau_L{}^b$/ps
pentanol	−20	16 815		654	722
	0	18 920	247	229	284
	20	18 100		119	123
	40	17 360	71	62	66
hexanol	−20	17 171		1056	1130
	0	17 115	373		429
	20	17 235	195	187	187
	40	17 484	87		95
heptanol	−20	17 523		1520	
	0	17 435	613	592	≈560
	20	17 585	234		255
	40	17 855	120		124
octanol	0	17 604		874	≈800
	20	17 760	347		353
	40	17 945	184		157

^{a} $\langle\tau_s\rangle = \sum_i A_i\tau_i/\sum_i A_i$. ^{b} From ref 38.

TABLE 2: Time Functions of the TRABS Spectra of 4 in Octanol

	short time		long time	
spectrum	*A*	τ/ps	*A*	τ/ps
early (decay)	0.62	79	0.38	338
late (rise)	0.44	68	0.56	399
emission (solvation)				349

D. Transient Absorption (TRABS) Measurements. From earlier measurements on compounds similar to **1**-**4** in this laboratory,[28,29,34] it was to be expected that the transient absorption bands remain relatively uninfluenced by solvation

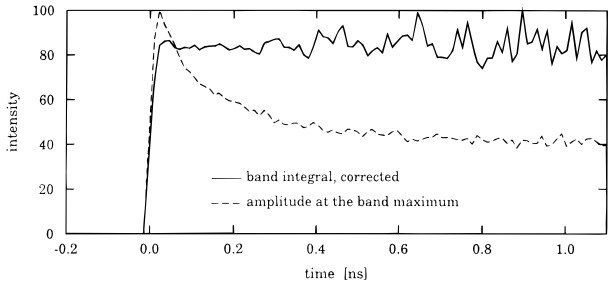

Figure 7. Population of the CT state during the solvation of **4** in hexanol: intensity of the band maximum as measured (- - -) and $\tilde{\nu}^3$-corrected band integral (—).

TABLE 3: Lifetimes of the Solvated CT States of 4 and 3

	compd **4** for solvents				compd **3**
	pentanol	hexanol	heptanol	octanol	hexanol
T, °C	τ/ns	τ/ns	τ/ns	τ/ns	τ/ns
0	13.40	15.42	17.04	17.97	29.86
20	14.02	15.88	17.41	18.24	29.16
40	14.70	16.52	17.93	18.67	28.64

and would merely reflect the actual electron transfer and the subsequent population decay of the CT state. The time dependence in those cases could be determined satisfactorily by band fitting with transient absorption spectra in *n*-hexane (marking the LE absorption) and in acetonitrile (marking the fully developed CT spectrum) or with an early and a late spectrum from the series of TRABS measurements (initial state and relaxed CT spectrum), respectively.[28,29,34] Such a fit procedure requires the applicability of a two-state reaction model and the supposition that the transient absorption spectra of the pure states do not change in shape and spectral position; they should vary in their intensity only. TRABS measurements on compound **4** have been carried out for comparison with this model. Furthermore, the question evolved whether the spectrum of the locally excited state can still be observed at early times.

As expected from Figure 8, top, we see that the TRABS spectrum of **4** in acetonitrile does not at all show the same form and position as the reference spectrum of Py^-.[32] The spectrum of **4** is broader and additionally slightly shifted to the red; however, the characteristic CT-band shape can be recognized. A significantly different result is obtained in *n*-hexane (Figure 8, top) where correspondence with the locally excited state of a suitable reference compound such as MePy is not seen: that spectrum is strongly shifted to the red and shows little structure. TRABS spectra in hexanol and octanol at room temperature exhibit the following characteristics (example octanol, displayed in Figure 8, bottom): following laser pulse excitation, the spectra change substantially. At no time can a spectrum be found which corresponds to the one obtained in the nonpolar solvent *n*-hexane. Though the position of the early spectra is similar to those in *n*-hexane, the bands are considerably less structured.

In Figure 8, bottom, it can well be recognized that the time-dependent shift of the absorption bands, the position, and the

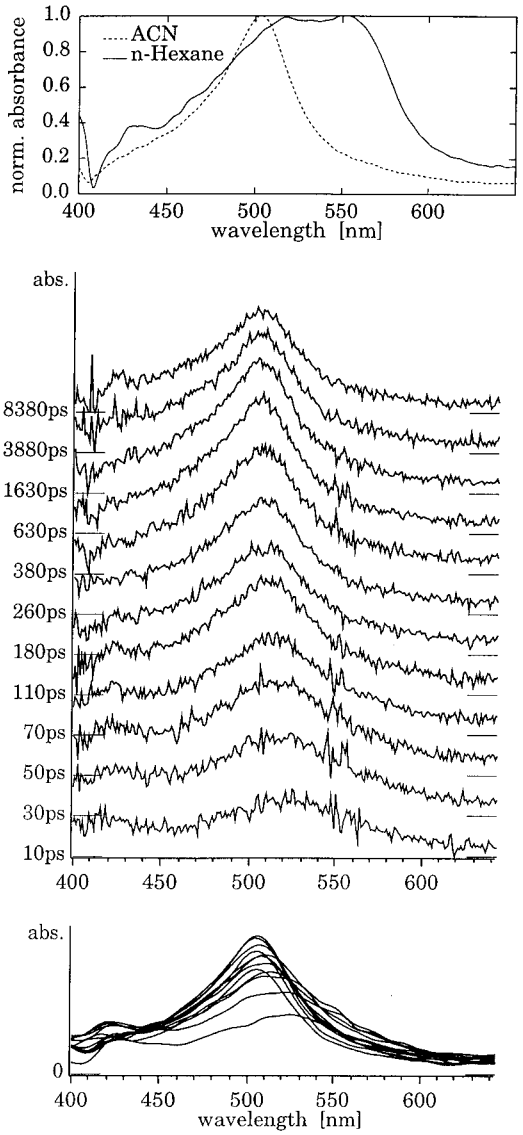

Figure 8. Transient absorption (TRABS) spectra of **4** at room temperature (23 °C). Top, in *n*-hexane, acetonitrile, 1 ns after excitation. Bottom: Time-resolved measurement in octanol.

band shape are accompanied also by a change of the intensity. Therefore, the band fit with the spectrum in *n*-hexane or a temporally early spectrum from the current series of measurements, as mentioned above, does not yield satisfactory results. The deviation between measurement and fit at the blue end of the spectrum is large, particularly at early times. Additionally, for an acceptable fit, a shift of the temporally late spectrum had to be adopted which varies in time and amounts to 15 nm at early times. Only in octanol was an (still) acceptable band fit obtained with a shift. The time functions thus obtained are not monoexponential (Figure 9, top). The intermediate time is shorter than τ_L, whereas the long time is close to τ_{L1}.

TABLE 4: CT Fluorescence Quantum Yield and Rates for Radiative (k_r) and Nonradiative (k_{nr}) Back Electron Transfer of 4 and 3

	compd **4**				compd **3**			
	Φ_{CT}	τ_{CT}/ns	$k_r/10^7$ s^{-1}	$k_{nr}/10^7$ s^{-1}	Φ_{CT}	τ_{CT}/ns	$k_r/10^7$ s^{-1}	$k_{nr}/10^7$ s^{-1}
pentanol	0.16	14.02	1.14	5.99				
hexanol	>0.18	15.88	1.13	5.16	0.38	29.16	1.30	2.13
heptanol	0.22	17.41	1.26	4.48				
octanol	0.20	18.24	1.10	4.39				
ACN	$<10^{-3}$	21			0.12	25	0.48	3.52
n-hexane	0.49[a]	20						

[a] See text.

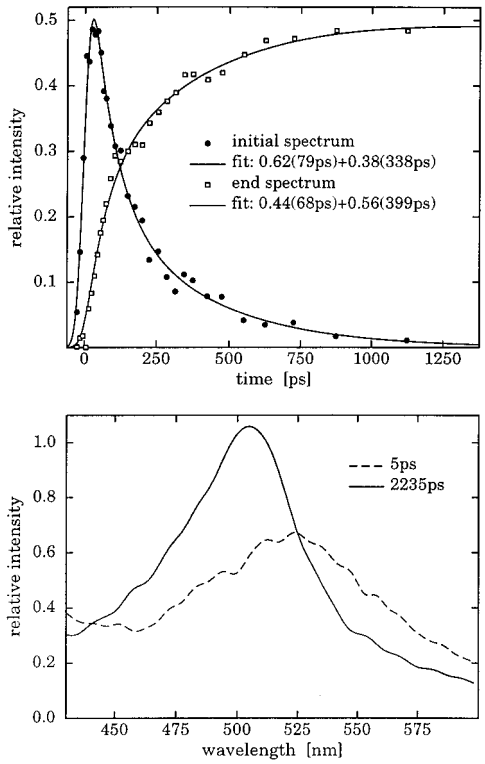

Figure 9. Fit of time functions of an early and a late transient absorption spectrum to the measured data of **4** in octanol (cf. Figure 8, bottom) at room temperature (23 °C). Top: Time evolution of the fitted amplitudes of the reference spectra. Bottom: Reference spectra.

The time-resolved emission spectra and the transient absorption spectra provide results which are contradictory if one adheres to the assumption that the absorption spectra are not influenced by solvation. If this assumption is abandoned for our molecule **4**, i.e., if the solvation process of the CT species in fact modulates the transient absorption spectrum, the charge separation would not be so clearly recognizable. This view is supported by the finding of a long decay and rise time, respectively, in absorption which is of the same order of magnitude as the value for the solvation found in the emission. It is therefore questionable whether the time constants (for the decay of the early and the rise of the late spectrum, respectively) calculated from the TRABS data actually reflect the electron-transfer reaction or instead merely exhibit τ_L. The lifetime of the solvent-relaxed CT state, as well as the rise time of the first excited triplet state, is not influenced by such effects since these times are much longer than τ_L.

E. Triplet Formation. In compounds **1** and **3** with freely rotating amino groups, the triplet state is populated from the CT state. This becomes manifest by the clearly visible triplet absorption spectrum (with a maximum at about 415 nm) a few nanoseconds after the excitation, whereby the rise time is identical with the decay time of the CT state.[29] In the case of compound **4**, such correspondence of rise and fall times is more difficult to prove since the triplet signal is much weaker. The final triplet yield of **4** is at most 30% of that of **3**, which is an upper limit due to the unknown amount of triplets which might have been generated directly from excited deteriorated solute molecules (the reduced photostability of **4** has already been mentioned above). The small triplet yield of **4** allows the inference to be drawn that, contrary to **3**, intersystem crossing from the CT state is not an important recombination channel in **4**.

F. Lifetime of the CT State. CT lifetime measurements have been carried out with the single-photon-counting correlation method. The results obtained at temperatures 0, 20, and 40 °C are listed in Table 3. The lifetime of the CT species increases (!) with increasing temperature (ca. 0.5 ns per 20 °C). This result is unexpected since the reference compound **3** shows the opposite temperature behavior (**3**: decrease is 0.5 ns per 20 °C). All measured decay times can be fitted quite well to a monoexponential function.

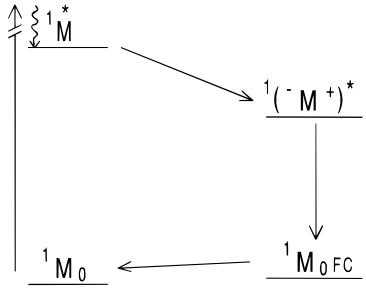

Figure 10. Reaction scheme for the supermolecule **4** showing the charge-separated state $^1(^-M^+)^*$ and the Franck−Condon ground state, M_{FC}.

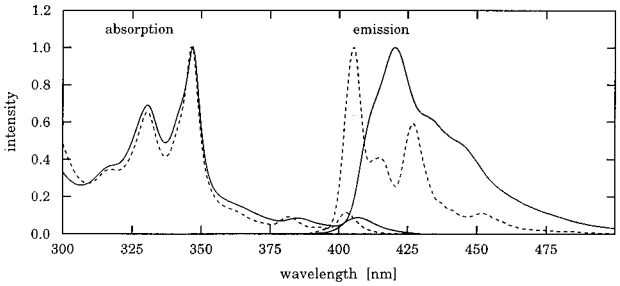

Figure 11. Normalized stationary absorption and emission spectra of **3** (- - -) and **4** (—) in *n*-hexane.

G. Quantum Yield of the Fluorescence. Data are listed in Table 4. Again, the reported quantum yields may be understated due to the possible existence of a deteriorated substance. The relatively low quantum yields of **4** suggest that the back electron transfer is predominantly radiationless. From Table 4, it is also apparent that the variation in the lifetime of the CT state can be explained primarily by the reduced rate of radiationless return electron transfer, with the rate for fluorescence, $k_r = \Phi/\tau_{CT}$, remaining nearly constant within the accuracy of the measurement. In contrast, the CT fluorescence quantum yields are larger for compound **3** for the same solvent (e.g., hexanol); a substantial fraction of the return electron transfer proceeds radiatively. A pronounced decrease of the fluorescence yield in **3** is also observed in ACN.

IV. Interpretation of the Results

The results lead to a reaction scheme for compound **4** as shown in Figure 10. After population of the excited state $^1M^*$, charge separation takes place within a time (probably in the subpicosecond range) which is shorter than the time resolution of the apparatus used in our study. The transition to the CT state $^1(^-M^+)^*$ of the supermolecule is therefore probably barrierless and the reaction strongly adiabatic, with the pyrenyl-like moiety being the electron-accepting part. A control of the electron-transfer rate by the solvent is not detectable.

Figure 11 shows emission bands in *n*-hexane which overlap with the red end of the absorption bands. The bands in the range at about 405 nm indicate the 0−0 transition of the S_1-S_0 absorption which is red-shifted by about 25 nm for **3** and **4** compared with MePy.

After the charge separation, solvation of the CT dipole, as depicted schematically in Figure 12, follows. The dipole

TABLE 5: Dielectric Data of Alcohols and Solvation Times of 4

		Debye times[a]			solvation times			τ_L times		comparison	
solvent	T, °C	τ_{D1}/ps	τ_{D2}/ps	τ_{D3}/ps	τ_{s1}/ps	τ_{s2}/ps	$\langle\tau_s\rangle$/ps	τ_L[b]/ps	τ_{LD1}[c]/ps	$\langle\tau_s\rangle/\tau_{L1}$	$\langle\tau_s\rangle/\tau_{LD1}$
PeOH	−20	6641			837	151	654	722	880	0.90	0.74
	0	2272			278	57	229	284	345	0.80	0.66
	20	927	28	2.7	162	51	119	123	150	0.96	0.79
	40	419	22	2.3	79	12	62	66	80	0.94	0.78
HxOH	−20	9939			1300	271	1056	1130	1376	0.93	0.77
	0	3212			373		373	429	535	0.87	0.70
	20	1210	31	2.9	205	31	187	187	225	1.00	0.83
	40	520	24	2.4	87		87	95	113	0.92	0.77
HpOH	−20				1830	267	1520				
	0				664	182	592	≈560		1.06	
	20	1465	34	3.2	234		234	255	305	0.92	0.77
	40	594	26	2.6	120		120	124	147	0.97	0.82
OcOH	0				977	262	874	≈800		1.09	
	20	1780	39	3.2	347		347	353	418	0.98	0.83
	40	668	29	2.7	184		184	157	184	1.17	1.00

[a] From refs 38, 39, and 42. [b] After eq 1. [c] After eq 2 with $\epsilon_c = 1$.

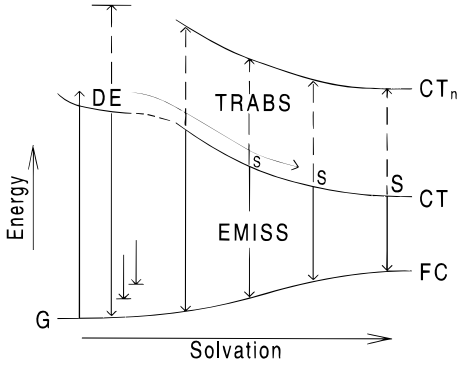

Figure 12. Scheme indicating the time evolution of the detectable transitions of **4** from the CT state during solvation: Stokes shift of the emission (EMISS), blue shift of the transient absorption (TRABS). G, ground state; FC, Franck−Condon ground state; DE, delocalized first excited singlet state, CT; CT$_n$, charge-transfer states.

(estimated dipole moment 25−30 D) is formed quasi-instantaneously. A slow development determined by the progressing solvation is not observed; a slow development would even contradict the time dependence of the integrated band intensity obtained after the $\tilde{\nu}^3$ correction (cf. Figure 7). A slow dipole formation would imply a change of the oscillator strength, which should entail a variation of the emission intensity as well. This is not the case here.

The transient absorption bands of **3** and **4** (cf. Figure 8) are influenced in their shape and spectral position by solvation, in contrast to previous transient absorption measurements on a similar class of short-linked A−D molecules investigated in this laboratory.[27c−29,32−34,41] Such changes due to solvation have also been reported for quite different molecular model systems (bis(*p*-aminophenyl) disulfide and its radical).[35] The results obtained in this respect with compound **4** represent the simplest case of transient absorption measurements, since no intramolecular conformation change occurs beyond solvation. For measurements of the other pyrene/DMA compounds of this series, such an influence of conformation changes is to be expected, e.g., as a blue shift of the transient absorption bands, an effect actually observed with compound **2** also. A separation of solvation effects from the effects due to intramolecular conformation changes is generally not possible, unless the solvation is considerably faster than the formation of the product to be measured (e.g., triplet formation).

An exact correspondence between the change of the TRABS spectra and the solvation dynamics cannot, however, be found because of the limited resolution of the absorption apparatus and the complicated spectra. The variation of the TRABS spectra may be attributed to a change of the energy distance between the first excited CT state and higher electronic CT states. An energy distance remaining constant during solvation would require that the dipole moment, μ_{CTn}, of the higher excited CT states be the same as that of the lowest excited CT state (μ_{CT}). This cannot be expected; rather, one has $\mu_{CTn} < \mu_{CT}$, resulting in a blue shift of the absorption bands. Additionally, a variation of the band shape is detected. This leads to the supposition that the development of the participating levels (probably avoided level crossing) does not change linearly with solvation. In that case, one would not expect conformity of the time functions for the band shift of absorption and emission.

A. Efficiency of Charge Separation. Compound **4** is a rather rigid and planar molecule having no possible significant intramolecular mobilities, such as rotation or translation. The TICT model (twisted intramolecular CT)[36,37] would therefore not predict a stable CT state, since according to this model an intramolecular rotation of a molecular group such as an amino group or a complete DMA derivative relative to the acceptor is required. In compound **4**, however, the amino group cannot rotate and the methylindoline moiety is rigidly connected to the pyrene. Nevertheless, the charge transfer is very efficient, like in another class of rigid A/D compounds,[1,2] and the lifetime of the relaxed CT state of 10 ns is also comparatively long. By contrast, the amino group in **3** can rotate, although the charge transfer is considerably slower than in **4**. At an early time in the spectrostreak measurements, the bands of the locally excited state can still be recognized. The subsequent solvation is therefore superimposed by the primary electron transfer and cannot be separated in time. These considerations lead to the conclusion that, at variance with the TICT model, free rotation of the amino group does not have a significant influence on the ability for electron transfer; rather, a planarly fixed amino group strongly enhances the ET efficiency here.

B. Solvation of the CT Band. Following the primary step of ET and the change of the dipole moment, a pure relaxation of the surrounding solvent takes place. The results reported in this work are essentially in agreement with the measurements by Barbara et al. in short linear alcohols.[14,15] Linear alcohols cannot be described by Debye behavior, such associating solvents showing nonlinear solvation dynamics. Only few data exist for the dielectric relaxation of alcohols. In particular, with longer chain alcohols, old data collected by Garg and Smyth (G−S)[38] might be considered in conjunction also with their temperature dependence (cf. Table 5). However, only the low-frequency data (leading to the longest relaxation time) from this

work seem sufficiently reliable. New data of fair quality but similar to the G−S results collected above 20 °C do exist.[39] The temperature behavior and the dependence on the structure of the solvent reflect the following considerations: At higher temperatures and with longer chain alcohols, the solvation time function could be fitted satisfactorily and more frequently by a monoexponential function. The accuracy of the times obtained, however, decreases with increasing temperature, and fast components of the solvation process, if present at all, may lie outside the possible fit range so that an equivocal clarification of the effect is not possible. The influence of the faster components of solvation is already recognized clearly. They are still absent in the measurements of similar decay times with longer alcohols. In the examples where a biexponential fit prevails, only in a few cases do short time components appear which correspond to the "second" relaxation time, τ_{D2} (as obtained from the intermediate dispersion region of the original microwave data of complex permitivities). Rather, the time components appear randomly distributed in the range between τ_{D2} and τ_{D1}. The question to which extent the second dispersion region contributes to the solvation behavior cannot be answered here. Furthermore, better data at a larger variety of temperatures for comparison are desired. Also, measurements of improved time resolution in short alcohols (methanol, ethanol) are necessary for a critical assessment of the influence of the chain length.

The best agreement with the reference data of τ_1 is the time defined as the mean solvation time $\langle\tau_s\rangle$, as is evident from Table 5. The deviations are only of the order of 10−15%. No improvement is obtained by calculating τ_{LD1} according to eq 2; a comparison with this time leads to a correlation with a factor of about 0.8. We also excluded the validity of the MSA theory for longer chain alcohols, since time components shorter than τ_L, as actually found here, should not appear according to this theory.

C. Lifetime of the CT State. Compound **3** in alcohol solution undergoes intersystem crossing from the CT state to the excited triplet state to a large extent; its transient absorption spectrum after some 10 ns is practically identical with the locally excited triplet state of pyrene. Such a clear-cut result, however, does not prevail in **4**. The triplet yield of **4** is considerably less than that of **3**; with respect to the observed small triplet signal, there exists the possibility that the largest fraction may come from the unavoidable photodegradation of the sample (perhaps intersystem crossing from a pyrenyl-like moiety). The lifetime of the CT state of both samples is temperature-dependent and also seems to be influenced by specific solvent properties. The CT lifetime of compound **4** rises with temperature, whereas the opposite effect is seen with compound **3**. Furthermore, the CT lifetime of **4** decreases with increasing solvent polarity. The quantum yield of the CT fluorescence of **3** is twice as large as that of **4**. From these results, the following conceivable explanation can be derived. Compound **3** has three deactivation channels for the CT state: the emission of a photon, intersystem crossing to the excited triplet state, and a radiationless return electron transfer (the latter process is of minor importance). The results are quite different with compound **4**: in alcohol solutions, only a small triplet formation is seen, and the quantum yield for emission is only half compared to **3**. The main channel for the deactivation is therefore a radiationless return electron transfer to the ground state. Due to the large free enthalpy, ΔG_{nr}, this reaction is expected to be in the "Marcus inverted region".[40] A temperature increase is connected with a decrease of the solvent polarity, which entails an increase of ΔG_{nr}. This leads to a decrease of the rate, k_{nr}. The analogous effect results upon variation of the solvent. The radiationless back transfer in **3** can be neglected, as pointed out above; the main channels in **3** are intersystem crossing and emission. The latter process is approximately temperature-independent (in the considered range between 0 and 40 °C), and the transition to the triplet state is expected to proceed in the "normal region" because of the small free-enthalpy change, ΔG_{isc}, involved. The rate k_{isc} will therefore rise with temperature, which results in a decrease of the lifetime of the CT state.

The model presented here, however, cannot fully explain the observed large differences in the CT-state lifetime of compound **4** upon variation of the solvent. Also, with the controlled variation of the temperature, the polarity (the bulk dielectric constant) of the solvents can be adjusted to be comparable. However, the measured corresponding rates differ widely. We presently assume the participation of specific solvent effects which require further investigations.

In the present work, we have also emphasized again, as in our earlier work,[34,27] that in strongly adiabatic CT reactions with "instantaneous" charge separation, the decay of the primary fluorescence will generally not provide data about the depopulation of the primarily excited state; rather, it will be determined by the Stokes-shift dynamics due to the solvation of the CT species; i.e., the early CT emission band moving away from the observation wavelength generates a "pseudo-decay" signal at the wavelength range where the initial (perhaps locally excited state) fluorescence is expected. spectrostreak measurements—although limited in time resolution by the time-smearing effect of the defraction grating[27]—reveal this phenomenon readily and clearly.

Acknowledgment. We thank J. Bienert, B. Frederichs, and H. Meyer for valuable technical assistance and Dipl. Chem. Simone Techert for discussions. This work has been supported in part by the Deutsche Forschungsgemeinschaft (DFG).

References and Notes

(1) (a) Oevering, H.; Verhoeven, J. W.; Paddon-Row, M. N.; Warman, J. M. *Tetrahedron* **1989**, *45*, 4751. (b) Verhoeven, J. W. *Pure Appl. Chem*. **1990**, *62*, 1585. (c) Oevering, H.; Paddon-Row, M. N.; Heppener, M.; Oliver, A. M.; Cotaris, E.; Verhoeven, J. W.; Hush, N. S. *J. Am. Chem. Soc*. **1987**, *109*, 3258. (d) Paddon-Row, M. N.; Oliver, A. M.; Warman, J. M.; Smit, K. J.; de Haas, M. P.; Oevering, H.; Verhoeven, J. W. *J. Phys. Chem*. **1988**, *92*, 6958. (e) Oliver, A. M.; Craig, D. C.; Paddon-Row, M. N.; Kroon, J.; Verhoeven, J. W. *Chem. Phys. Lett*. **1988**, *150*, 366.

(2) (a) Wasielewski, M. R.; Niemczyk, M. P.; Johnson, D. G.; Svec, W. A.; Minsek, D. W. *Tetrahedron* **1989**, *45*, 4785. (b) Rettig, W.; Haag, R.; Wirz, J. *Chem. Phys. Lett*. **1991**, *180*, 216.

(3) Bagchi, B.; Oxtoby, D. W.; Fleming, G. W. *Chem. Phys*. **1984**, *86*, 257.

(4) Van der Zwan, G.; Heynes, J. T. *J. Phys. Chem*. **1985**, *89*, 4181.

(5) Chandra, A.; Bagchi, B. *Chem. Phys. Lett*. **1988,** *151*, 47.

(6) Nichols, A. L.; Calef, D. F. *J. Chem. Phys*. **1988**, *89*, 3783.

(7) Wolynes, P. *J. Chem. Phys*. **1987**, *86*, 5133.

(8) Rips, I.; Klafter, J.; Jortner, J. *J. Chem. Phys*. **1988**, *89*, 4288.

(9) Onsager, L. *Can. J. Chem*. **1977**, *55*, 1819.

(10) Van der Zwan, G.; Heynes, J. T. *Phys*. **1983**, *121A*, 227.

(11) Van der Zwan, G.; Heynes, J. T. *Chem. Phys. Lett*. **1983**, *101*, 367.

(12) Maroncelli, M.; Fleming, G. R. *J. Chem. Phys*. **1987**, *86*, 6221.

(13) Declemy, A.; Rullière, C. *Chem. Phys. Lett*. **1988**, *146*, 1.

(14) Kahlow, M. A.; Jarzeba, W.; Kang, T. J.; Barbara, P. F. *J. Chem. Phys*. **1989**, *90*, 151.

(15) Jarzeba, W.; Walker, G. C.; Johnson, A. E.; Barbara, P. F. *Chem. Phys*. **1991**, *152*, 57.

(16) Kivelson, D.; Madden, P. *J. Phys. Chem*. **1984**, *88*, 665.

(17) Friedrich, V.; Kivelson, D. *J. Chem. Phys*. **1987**, *86*, 6425.

(18) Kirkwood, J. G. *J. Chem. Phys*. **1934**, *2*, 351.

(19) Weisenborn, P. C. M.; Huizer, A. H.; Varma, C. A. G. O. *Chem. Phys*. **1989**, *133*, 437.

(20) Vollmann, H.; Becker, H.; Corell, M.; Streek, H. *Liebigs Ann. Chem*. **1937**, *531*, 1.

(21) Clar, *E. Chem. Ber*. **1948**, *81*, 524.

(22) Jutz, C. H.; Kirchlechner, R.; Seidel, H. J. *Chem Ber*. **1969**, *102*, 2301.

(23) Jensen, A.; Berg, A. *Acta Chem. Scand*. **1965**, *19*, 1838.

(24) Dickermann, S. C.; Feigenbaum, W. M. *Chem. Commun*. **1966**, 345.

(25) Reynders, P.; Kühnle, W.; Zachariasse, K. A. *J. Am. Chem. Soc*. **1990**, *112*, 112.

(26) According to Burfield et al. (Burfield, D. R.; Lee, K. H.; Smithers, R. H. *J. Org. Chem.* **1977**, *42*, 3060) optimal drying of acetonitrile over P_4O_{10} for 1 day yields 9 ppm of water: i.e., 5×10^{-4} mol/L of H_2O compared typically to 1×10^{-5} mol/L of the desolved compound **4**. The literature values for alcohols are found in: Burfield, D. R.; Smithers, R. H. *J. Org. Chem*. **1983**, *48*, 2420. *n*-Alcohols (Fluka, purissimum) used in the present work were dried over molecular sieve (3 Å) and distilled under vacuum.

(27) (a) Wiessner, A.; Staerk, H. *Rev. Sci. Instrum.* **1993**, *64*, 3430. (b) Staerk, H.; Wiessner, A.; Müller, C.; Mohr, J. *Rev. Sci. Instrum*. **1996**, *67*, 2490. (c) Wiessner, A. Dissertation, Univ. Göttingen, 1994.

(28) Hüttmann, F.; Kühnle, W.; Staerk, H. *J. Photochem. Photobiol., A: Chem*. **1993**, *70*, 83.

(29) Hüttmann, G. Dissertation, Univ. Göttingen, 1992. Techert, S. Doctoral work, in progress.

(30) (a) Melhuish, W. H. *Natl. Bur. Std. 378, Proc. Conf. NBS, Gaithersburg* **1972**, 378. (b) Velapoldi, R. A. *Natl. Bur. Std. 378, Proc. Conf. NBS, Gaithersburg* **1972**, 138.

(31) Marcus, R. A. *J. Phys. Chem*. **1989**, *93*, 3078.

(32) Shida, T. *Electronic Absorption Spectra of Radical Ions*; Physical Science Data; Amsterdam, 1988; Vol. 34.

(33) Wiessner, A. Diplomarbeit, Univ. Göttingen, 1991.

(34) Wiessner, A.; Hüttmann, G.; Kühnle, W.; Staerk, H. *J. Phys. Chem*. **1995**, *99*, 14923.

(35) Ernsting, N. P. *Chem. Phys. Lett*. **1990**, *166*, 221.

(36) Grabowski, Z. R.; Rotkiewicz, K.; Siemiarczuk, A.; Cowley, D. J.; Baumann, W. *Nouv. J. Chem*. **1979**, *3*, 443.

(37) Rettig, W. *Angew. Chem*. **1986**, *98*, 969.

(38) Garg, S. K.; Smyth, C. P. *J. Phys. Chem*. **1965**, *69*, 1294.

(39) Gestblom, G.; Sjöblom, J. *Acta Chem. Scand*. **1984**, *A38*, 47.

(40) Marcus, R. A. *J. Chem. Phys*. **1956**, *24*, 966.

(41) Petrov, N. Kh.; Wiessner, A.; Fiebig, T.; Staerk, H. *Chem. Phys. Lett.* **1995**, *241*, 127. In that work, the probe molecule was 8-*N*,*N*-(dimethylamino)-11*H*-indeno[2,1-*a*]pyrene (identical with compound **3** in the present study) and not 4,5-(1′-methylindolino)-3*H*-4,5-benzonaphthanthracene; see also the Experimental Section, synthesis and characterization.

(42) Su, S.-G.; Simon, J. D. *J. Chem. Phys*. **1988**, *89*, 908.